Molecular Crystals and Liquid Crystals
Publication details, including instructions for authors and subscription information:
http://www.tandfonline.com/loi/gmcl20

Comparison of Polypyrrole Organic Thin Film Actuators with or without Silicon Microspring

Yutaro Suzuki [a], Shou Ogihara [a], Daiki Hoshino [a], Tsuyoshi Morita [a], Yutaka Chida [a], Hiroyuki Katsumata [a], Takayuki Fujiya [a], Zongfan Duan [a] & Yasushiro Nishioka [a]

[a] Department of Precision Machinery Engineering, College of Science and Technology, Nihon University, Funabashi, Chiba, Japan

Version of record first published: 16 May 2011

To cite this article: Yutaro Suzuki, Shou Ogihara, Daiki Hoshino, Tsuyoshi Morita, Yutaka Chida, Hiroyuki Katsumata, Takayuki Fujiya, Zongfan Duan & Yasushiro Nishioka (2011): Comparison of Polypyrrole Organic Thin Film Actuators with or without Silicon Microspring, Molecular Crystals and Liquid Crystals, 539:1, 148/[488]-155/[495]

To link to this article: http://dx.doi.org/10.1080/15421406.2011.566112

Mol. Cryst. Liq. Cryst., Vol. 539: pp. 148/[488]–155/[495], 2011

ISSN: 1542-1406 print/1563-5287 online
DOI: 10.1080/15421406.2011.566112

Taylor & Francis
Taylor & Francis Group

Comparison of Polypyrrole Organic Thin Film Actuators with or without Silicon Microspring

YUTARO SUZUKI, SHOU OGIHARA, DAIKI HOSHINO, TSUYOSHI MORITA, YUTAKA CHIDA, HIROYUKI KATSUMATA, TAKAYUKI FUJIYA, ZONGFAN DUAN, AND YASUSHIRO NISHIOKA

Department of Precision Machinery Engineering, College of Science and Technology, Nihon University, Funabashi, Chiba, Japan

Organic actuators utilizing electrochemomechanical strain are of special interest for application in some types of microelectromechanical systems (MEMS). Amongst of those, polypyrrole (PPy) actuators have advantages of their large strain and stress. In this work, two kinds of PPy thin film actuators with or without a silicon MEMS microspring were fabricated and compared. The polypyrrole thin films with the thickness of 91 μm were deposited by galvanostatic electropolymerization. One of the actuators was inserted with a silicon MEMS microspring with the length of 15 mm, the width of 0.5 mm, and the thickness of 60 μm. The MEMS PPy actuator exhibited nearly 12% of the electrochemical strain under the load stress of 0.3 MPa in a water solution of an electrolyte, lithium bis-trifluoromethane sulphonyl imide (LiTFSI) at the bias sweeping rate of 10 mV/s in the voltage range between −1 and 1 V. Although the performances of the MEMS acstuators showed some degradation compared to the PPy actuator without the MEMS microspring, the MEMS PPy actuator may be beneficial to drive MEMS structures, which require a large strain and a large stress with a low voltage actuation.

Keywords Electrochemomechanical; linear actuator; MEMS; polypyrrole; silicon

1. Introduction

Recent reports on organic soft linear actuators made of conducting polymers such as polypyrrole (PPy) films are very interesting because they have fairly large electrochemical stresses between 3 and 5 MPa [1–5]. Their strains were between 1 to 3%. Recently, it has been reported that some PPy actuators exhibited strains of more than 10% [5–9], and that some of those achieved up to 40% of strain [9]. The improved strain has been mostly achieved using an electrolyte of tetra-n-butylammonium

Address correspondence to Yasushiro Nishioka, Department of Precision Machinery Engineering, College of Science and Technology, Nihon University, 7-24-1 Narashinodai, Funabashi, Chiba 274-8501, Japan. Tel.: +81-47-469-6482; Fax: +81-47-469-6482; E-mail: nishioka@eme.cst.nihon-u.ac.jp

bis(trifluoromethansulfonyl)imide (TBATFSI) during PPy electropolymerization. These actuators generally function under a low potential voltage less than 1 V. These researches have mostly concentrated on improving the PPy film performances by optimizing electroplymerization conditions.

Recently, Ding *et al.* reported a new type of PPy actuator that had a tubular geometry and a helical wire interconnect [10]. The actuator was fabricated by forming a PPy film on a platinum wire (125 μm in diameter) that was wrapped around with thinner (25 μm in diameter) platinum wire. A maximum strain of 5% and the response of $10\%s^{-1}$ were achieved. A similar structure to minimize the response time of PPy actuators was also reported by Hara *et al.* [11–14]. They deposited a PPy film on a tungsten helical coil (250 μm in diameter) made of a tungsten wire with a diameter of 30 μm. This fibrous PPy actuator exhibited a strain of 11.6% under the load of 0.2 N. The tungsten wire also helped to reduce the potential drop within the PPy for the improved performance. Another trial to increase the extension and contraction ratios employing a corrugated PPy structure has been reported [15], and a bimorph structure of a PPy actuator for more uniform bending has also been reported [16].

In contrast, we considered applying these PPy soft actuator techniques to the actuation of the very small mechanisms used in silicon microelectromechanical systems (MEMS). To the best of our knowledge, there have been very few applications of these techniques to the actuation of small MEMS mechanisms. In this paper, two kinds of PPy thin film actuators with or without a silicon MEMS microspring were fabricated and compared.

2. Linear Actuator Design

Figure 1 describes the designed actuator. The silicon microspring has a width of 0.5 mm, length of 15 mm, and thickness of 60 μm. The microspring consists of silicon wires having a cross-section of $10 \times 60\,\mu m^2$. The surface of this microspring is covered by a 91 μm-thick PPy film of length and width 15 mm and 7 mm, respectively. The PPy film covering the microspring shrinks and expands along with the PPy film beside the microspring, which causes the actuation of the microspring. The top and bottom parts of the actuator were clipped with metal electrodes. As a result, the

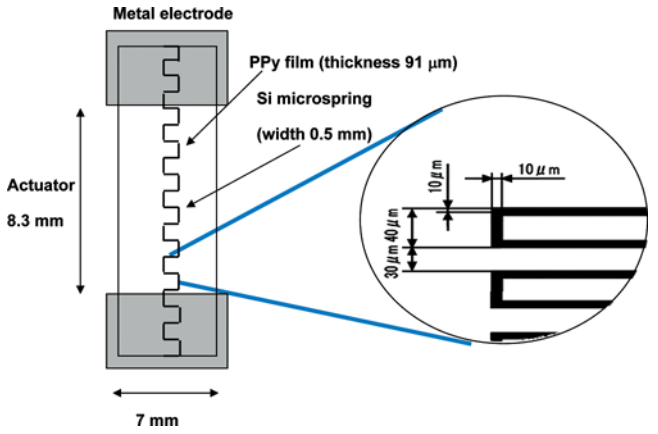

Figure 1. Design of the PPy-driven silicon linear actuator; (a) corresponds to designed silicon microspring, and (b) corresponds to the designed linear actuator driven by PPy expansion and contraction motions.

working area of the actuator was 8.3 mm in length and 7 mm in width. A PPy actuator with the same dimensions without the silicon MEMS microspring was also fabricated for comparison.

3. Actuator Fabrication Processes

Figure 2 describes the fabrication processes of the microactuator. First, an extremely thin (60 μm) silicon film was anodically bonded to a glass substrate of 1.5 mm in thickness (a). Next, the silicon microspring pattern was photolithographycally defined on the silicon film, followed by silicon etching using an inductively coupled plasma (ICP) dry etcher (b). The silicon microspring was released by immersing the structure in a buffered HF solution (c). The microspring was placed on an acrylic board, and a 100 nm-thick Au film was sputter deposited on the whole surface of the microspring and the acrylic board (d). Finally, the PPy film with a thickness of approximately 91 μm was electrochemically deposited on the whole surface of the sputtered Au film, and the structure was peeled off from the acrylic board in acetone (e).

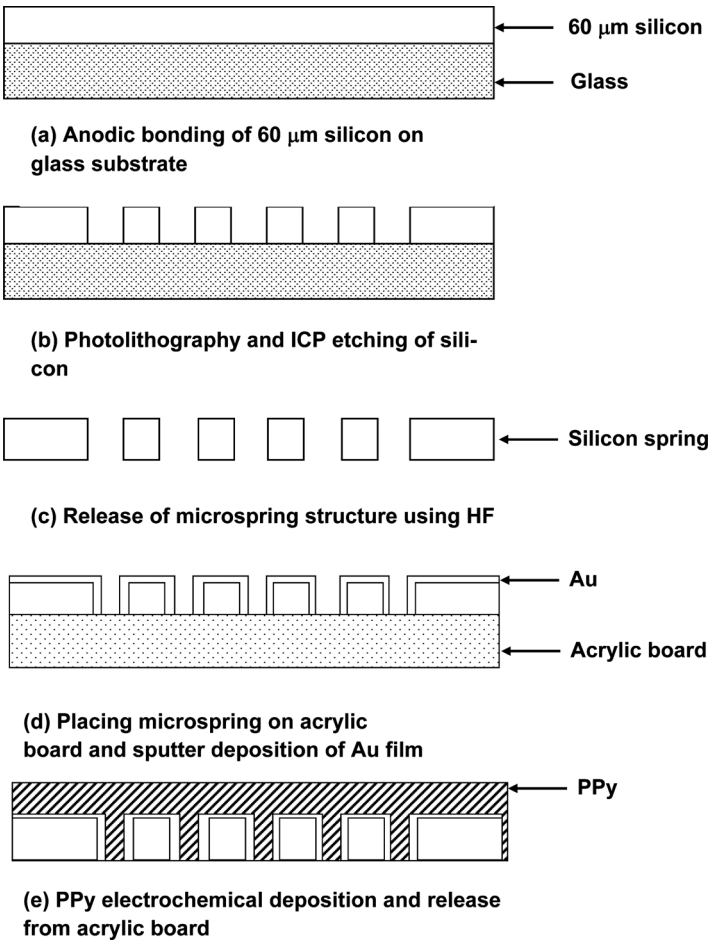

Figure 2. Cross-sectionally described linear actuator fabrication processes.

The polymerization was done using a computer-controlled potentio-galvanostat (Hokuto Denko HZ-5000). A counter electrode (Ti), a reference electrode (Ag/AgCl), and a working electrode (Au) were immersed into a solvent containing pyrrole monomers and an electrolyte, and the potential voltage was controlled to keep a constant current between the counter electrode and the working electrode of the Au surface covering the silicon microspring during the PPy polymerisation. The electropolymerization of PPy was done in a methyl benzoate solution with a volume of 50 ml in which pyrrole monomers with a concentration of $0.25\,\mathrm{mol}\cdot\mathrm{dm}^{-3}$ and the electrolyte tetra-n-butylammonium bis(trifluoromethansulfonyl)imide (TBATFSI) with a concentration of $0.2\,\mathrm{mol}\cdot\mathrm{dm}^{-3}$ are dissolved. The polymerization was done at a constant current density of $0.2\,\mathrm{mA}\cdot\mathrm{cm}^{-2}$ for 4 h at room temperature. The PPy film deposited on the Au surface was peeled off, and cut into the actuator dimension of $7\times15\,\mathrm{mm}^2$ as shown in Figure 3(b). The PPy actuator without the Si microspring of $7\times15\,\mathrm{mm}^2$ was also cut from the same PPy film. The thickness of the plane part of the PPy film was measured to be approximately 91 μm using a micrometer. The measured electro conductivity of the PPy film was approximately $12\,\mathrm{Scm}^{-1}$. In the previous publications, fairly large strain and fast response of PPy actuators, that were polymerized electrochemically with TBATFSI at the temperature of −10°C, were reported [5–14]. Therefore, the PPy actuators fabricated using (TBATFSI) were focused in this research.

Figure 3 shows the optical microscope image of the fabricated actuator taken from the backside (substrate side) of the actuator. The Au film in the plane PPy area was unintentionally peeled off from the PPy film during the actuator peeling off process in acetone, while the Au film covering the silicon microspring was not peeled off. Figure 4(a) and 4(b) show scanning electron microscope (SEM) images of the PPy actuator observed from the surface of the microspring (electrolyte solution side) and the backside of the microspring, respectively. It was indicated that the PPy film almost covered the silicon spring surface, and it had a rugged surface structure. Similar rugged structures were observed in the image taken from the backside. It is believed that this sponge-like structure is the origin of the large expansion and contraction ratios during the ion doping and dedoping processes. The space between the microsprings was not filled with the PPy film. This may mean that the polypyrrole

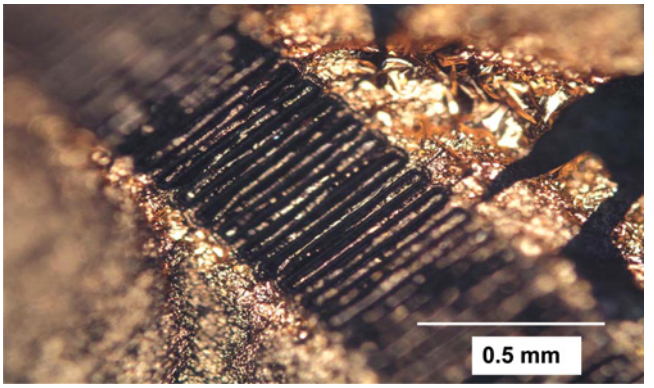

Figure 3. Optical microscope image of the fabricated actuator taken from the backside (substrate side) of the actuator. The Au film in the plane PPy area was peeled off, while the Au film covering the silicon microspring was not peeled off.

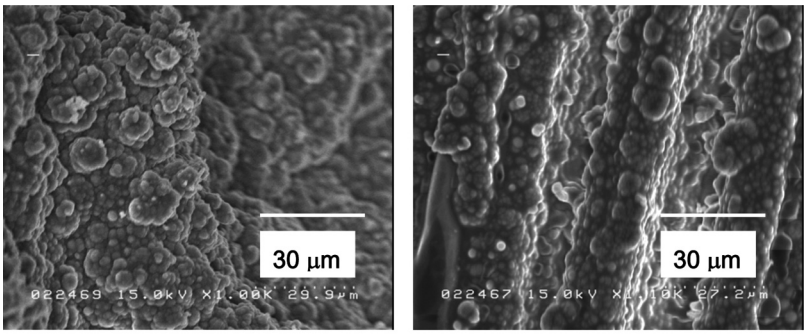

Figure 4. Electron microscope (SEM) images of the PPy actuator observed from the surface (electrolyte solution side) of the microspring (a) and backside 8 substrate side) of the microspring (b).

film on the microspring does not contribute the extension and contraction of the silicon actuator. Therefore, it was determined that the actuation was realized utilizing the extension and contraction of the plane PPy film deposited beside the microspring.

4. Characterizations

The actuator characterization system that utilizes a balance to measure the expansion and contraction ratios under the load stress has already been described in the previous publications [15,16]. The PPy actuator was used as the working electrode in the lithium bis(trifluoromethansulfonyl)imide (LiTFSI) electrolyte solution of $1\,\mathrm{mol}\cdot\mathrm{dm}^{-3}$, and both of the PPy actuator ends were suspended by metal clips. The size of the moving part of the PPy actuators was 7 mm in width, 8.3 mm in length, and 91 μm in thickness. The PPy actuator exhibited the expansion and contraction motions under the alternating potential with the triangular wave shape applied between the PPy actuator and the counter electrode. The potential voltage difference between the PPy actuator and the electrolyte solution was monitored using an Ag/AgCl reference electrode. The peak values of the potential voltage were -1 and $+1$ V, and the potential sweep rate was $10\,\mathrm{mVs}^{-1}$. The extension and contraction of the PPy actuator was measured by monitoring the displacement of the weight position using the laser displacement sensor. An arbitrary load stress was applied on the PPy actuator by putting weights on the saucer of the balance. The weights used here were 0.05, 0.2, and 0.5 N. The load stresses for these weights correspond to 0.07, 0.3, and 0.76 MPa, respectively.

Figure 5 shows the time dependences of the displacement (length change) of the actuators as measured with different weights of (a) 0.05 N, (b) 0.2 N, and (c) 0.5 N for the initial period of 800 seconds. Those weights correspond to 0.07, 0.3 and 0.76 MPa, respectively. The displacement vs. time curve for the eight of 0.05 N [Fig. 5(a)] seems to consist of two components of the electrochemical strain caused by the anion doping/dedoping processes and the creeping strain possibly due to the swelling of the PPy film. Here, the peak hight was subtracted by the creeping strain and as shown in Figure 5(a), and the subtracted peak hight value was divided by the initial length of the actuator to define the electrochemical strain. In this case

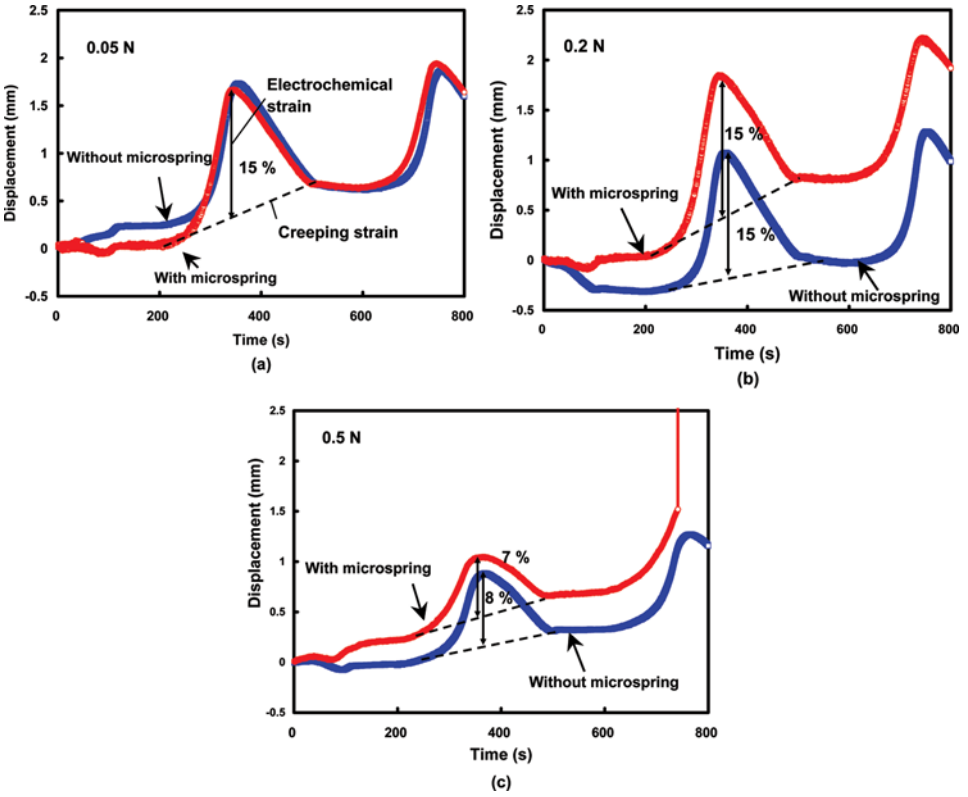

Figure 5. Time dependences of the displacement (length change) of the actuators as measured with different weights of (a) 0.05 N, (b) 0.2 N, and (c) 0.5 N for the initial period of 800 seconds. Those weights correspond to 0.07, 0.3 and 0.76 MPa, respectively.

of the weight of 0.05 N (0.07 MPa), the electrochemical strains of the PPy actuators with or without the silicon microspring are nearly identical. In contrast, when the weight increased up to 0.2 N (0.3 MPa), the creeping strain of the PPy actuator with the silicon microspring increased notably, while the electrochemical strains of two actuators are nearly identical as seen in Figure 5(b). When the 0.5 N (0.76 MPa) was applied, both of the actuators showed the smaller electrochemical strains of approximately 7–8%. In addition, the PPy actuator with the microspring torn off while the PPy actuator without the microspring did not tear off. The optical microscope observation of the torn off actuator showed cracks at the spring/PPy interface. The reason for the reduced electrochemical strain in the high load stress is not clear. The stressed polymer networks might possibly block the volume expansion caused by penetration of anions.

Figure 6 shows the repeated operation of the actuator for 15 times. The displacement of the actuators gradually increased due to creeping, while the electrochemical strains of them slightly decreased. The actuator with the microspring continued to have the electrochemical strain of 13%, while the actuator without the microspring continued to have that of 15%. The creeping effect of the PPy actuator with the silicon microspring was larger than the PPy actuator without the silicon microspring.

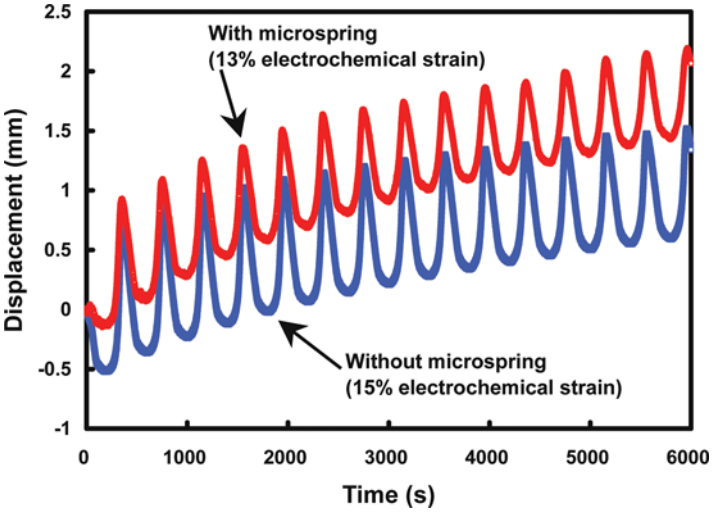

Figure 6. Relationships between the displacement of the actuators and time under the repeated operation of the actuator for 15 times. The load weight was 0.2 N that corresponds to 0.3 MPa stress.

Although the PPy actuator with the silicon microspring had sightly degraded performances compared to the PPy actuators without the silicon microspring, it will be beneficial for MEMS applications because of its large stress and strain.

The length of the actuator continues to increase as time elapses. This behaviour looks similar to the creeping effect in metal deformation processes. Zama and others recently reported on their detailed study for this creeping effect of PPy actuators, and concluded that this elongation could be recovered by releasing the stress during the deformation [17–19].

Although the actuator investigated here exhibited a slow response, the generating stress of the order of 0.3 MPa is relatively large as an actuating mechanism for MEMS actuation. The PPy actuator requires an electrolyte solution during actuation. Therefore, some protecting film such as an artificial skin to cover the electrolyte solution surrounding the PPy actuator may be needed for actual MEMS applications.

5. Conclusion

Two kinds of PPy thin film actuators with or without the silicon MEMS microspring were fabricated and compared. The polypyrrole thin films with the thickness of 91 μm were deposited by galvanostatic electropolymerization of a polypyrrole thin film using a methyl benzoate electrolyte solution of tetra-n-butylammonium bis(trifluoromethansulfonyl)imide (TBATFSI). One of the actuators was inserted with the silicon MEMS microspring with the length of 15 mm, the width of 0.5 mm, and the thickness of 60 μm. The MEMS PPy actuator exhibited nearly 12% of the electrochemical strain under the load of 0.2 N in a water solution of an electrolyte, lithium bis-trifluoromethane sulphonyl imide (LiTFSI) at the bias sweep rate of 10 mVs^{-1} in the voltage range between −1 and 1 V. The load stress was approximately 0.3 MPa. Although the performances of the MEMS actuators showed some degradation com-

pared to the PPy actuator without the MEMS microspring, the MEMS PPy actuator may be beneficial to drive MEMS structures, which require a large strain and a large stress with a low voltage actuation.

Acknowledgment

The devices investigated in this work were fabricated in the Micro Functional Device Research Center of the College of Science and Technology, Nihon University.

References

[1] Baughman, R. H. (1996). *Synth. Met.*, *78*, 339.
[2] Della Santa, A., & De Rossi, D., & Mazzoldi, A. (1997). *Synth. Met.*, *90*, 93.
[3] Kaneko, M., Fukui, M., Takashima, W., & Kaneto, K. (1997). *Synth. Met.*, *84*, 795.
[4] Madden, J. D., Cush, R. A., Kanigan, T. S., Brenan, C. J., & Hunter, I. W. (1999). *Synth. Met.*, *105*, 61.
[5] Hutchison, A. S., Lewis, T. W., Moulton, S. E., Spinks, G. M., & Wallace, G. G. (2000). *Synth. Met.*, *113*, 121.
[6] Kaneto, K., Sonoda, Y., & Takashima, W. (2000). *Jpn. J. Appl. Phys.*, *39*, 5918.
[7] Bay, L., West, K., Sommer-Larsen, P., Skaarup, S., & Benslimane, M. (2003). *Adv. Mater.*, *15*, 310.
[8] Hara, S., Zama, T., Takashima, W., & Kaneto, K. (2004). *Polym. J.*, *36*, 151.
[9] Zama, T., Hara, S., Takashima, W., & Kaneto, K. (2004). *Bull. Chem. Soc. Jpn.*, *77*, 1425.
[10] Ding, J., Liu, L., Spinks, G. M., Zhou, D., Wallace, G. G., & Gillespie, J. (2003). *Synth. Met.*, *138*, 391.
[11] Hara, S., Zama, T., Takashima, W., & Kaneto, K. J. (2004). *J. Mater. Chem.*, *14*, 1516.
[12] Hara, S., Zama, T., Takashima, W., & Kaneto, K. (2004). *Polym. J.*, *36*, 933.
[13] Hara, S., Zama, T., Sewa, S., Takashima, W., & Kaneto, K. (2003). *Chem. Lett.*, *32*, 800.
[14] Hara, S., Zama, T., Takashima, W., & Kaneto, K. (2004). *Synth. Met.*, *146*, 47.
[15] Morita, T., Chida, Y., Hoshino, D., Fujiya, T., & Nishioka, Y. (2010). *Mol. Cryst. Liq. Cryst.*, *519*, 121.
[16] Chida, Y., Morita, T., Machida, R., Hoshino, D., & Nishioka, Y. (2010). *Mol. Cryst. Liq. Cryst.*, *519*, 115.
[17] Zama, T., Hara, S., Takashima, W., & Kaneto, K. (2005). *Jpn. J. Appl. Phys.*, *44*, 8153.
[18] Zama, T., Hara, S., Takashima, W., & Kaneto, K. (2005). *Synth. Met.*, *149*, 199.
[19] Sendai, T., Suematsu, H., & Kaneto, K. (2009). *Jpn. J. Appl. Phys.*, *48*, 51506.